Proceedings of the Korean Nuclear Society Spring Meeting

Cheju, Korea, May 2001

Thermal-Hydraulic Behavior of Multiple U-Tubes in a Reflux Condensation Mode

Kyung-Won Lee, Moon-Hyun Chun, In-Cheol Chu*, Kyong-Won Seo

Korea Advanced Institute of Science and Technology

373-1, Kusong-Dong, Yusong-Gu, Taejon, 305-701, Korea

Sang-Jun Ha

Korea Electric Power Research Institute

103-16, Munji-Dong, Yusong-Gu, Taejon, 305-380, Korea

ABSTRACT

A series of experiments were performed to investigate the thermal-hydraulic phenomena inside the steam generator U-tubes in a reflux condensation mode. A total of 512 data for local condensation heat transfer coefficients (108 for pure steam flow and 404 for steam-air flow conditions, respectively) have been obtained for various inlet flow rates of steam and air under atmospheric condition. A new correlation, which includes the effects of flow rates of steam and noncondensible gases (air) on the heat transfer coefficient and is applicable to the reflux condensation mode, has been developed using the concept of degradation factor based on the steam-air experimental results. In addition, the effect of multiple U-tubes with different lengths (i.e., two-long and two- short U-tubes) on the onset of flooding during a reflux condensation has been examined.

1. INTRODUCTION

Reflux condensation cooling operation is one of alternative operation modes when a residual heat removal system is lost during the mid-loop operation or small-break loss of coolant accident (SBLOCA) in a PWR and it plays an important role in the core cooling. During the reflux condensation cooling operation, three distinctive modes may occur in the steam generator (S/G) U-tubes depending on the operating conditions: In filmwise reflux condensation mode, a vertical countercurrent flow of steam and condensate is formed in S/G U-tubes upflow side, whereas in the oscillatory (or total reflux condensation) mode, when the riser section of U-tube is blocked by a single phase-liquid column formed above the two-phase region, the reactor primary coolant may be decreased. And in natural circulation (or carry-over) mode, on the other hand, the liquid column can be carried over to the other side of U-tube and the steam flows cocurrently with its condensate.

In the safety analysis of nuclear power plants during the reflux condensation, it is very important to

* Korea Atomic Energy Research Institute
150, Dukjin-Dong, Yusong-Gu, Taejon, 305-353, Korea

determine the mechanisms governing heat transfer phenomena and to investigate the factors affecting the onset of flooding in S/G U-tubes during the reflux condensation. Therefore, the thermal-hydraulic phenomena in U-tubes during a reflux condensation have been extensively studied both experimentally and theoretically by Calia, C. and Griffith, P.(1982), Nguyen, Q. T. and Banerjee, S. (1982), Banerjee et al. (1983), Wan et al. (1983), and Chun, M. H. and Park, J. W. (1984) since 1980s, and more recently by Girard and Chang (1992), Noel, B. and Deruaz, R. (1994), Chen et al. (1999) and Moon et al. (2000). A larger scale experiment has also been carried out at several integral test facilities, such as LSFT (Kukita et al., 1988), BETHSY (Dumont et al., 1994), and IIST (Lee et al., 1996).

Although numerous studies on the reflux condensation in scaled down and full-scale facilities have already been conducted, no experimental data are currently available in open literatures that show the local heat transfer phenomena in U-tube upflow side during filmwise reflux condensation mode and/or the effect of multiple U-tubes on the onset of flooding. The main purpose of this work is to evaluate the local condensation heat transfer with and without noncondensible gases and to investigate the effect of multiple U-tubes on the onset of flooding during a reflux condensation. In addition, the present study is aimed at the quantification of the effects of S/G secondary side pool temperature and the flow rates of steam and noncondensible gases (air) on the heat transfer phenomenon.

2. EXPERIMENTS

2.1 Experimental Apparatus

A schematic diagram of the experimental apparatus is shown in Fig. 1. The main components of the system were ① the test section, ② the steam and air supply system, ③ sensors and devices to measure the temperature and flow rates, and ④ the data acquisition system.

In the present study, five U-tubes with the same inner diameter of 0.0162m are installed in a rectangular pool ($314.4 \times 117.2 \times 3600$ mm^3) as shown in Fig.1. The U-tubes have three different height steps with a triangular array as can be seen in Figs.1 (a) and (b). The heights of two outer U-tubes, one central U-tube, and two inner U-tubes are 3.3 m, 2.8 m, 2.5 m, respectively. The height of inner U-tubes are adjustable so that the effect of height difference on the thermal-hydraulic behavior can be investigated. The central U-tube is fully equipped with 32 thermocouples (shown in Figs.1 (c) and (d)) to evaluate the heat transfer coefficients, whereas outer U-tubes are used to investigate the effect of multiple U-tubes on the flooding phenomena.

Steam, which was supplied by a 200 kW electric steam boiler, passes through two steam-water separators, a flow control needle valve, and an accurately calibrated turbine flow meter before it finally flows into the test section. Two steam-water separators were provided to supply sufficiently dry saturated or slightly superheated steam to the test section.

Air, on the other hand, was supplied from a central air supply system of the KAIST. The preheater made it possible to maintain the air temperature at a constant level equal to the steam temperature. The flow rate of air is controlled by a needle valve and measured by a rotameter.

2.2 Test Parameters and Test Procedure

The controllable test parameters were the pool temperature of the S/G secondary side and the inlet flow rates of steam and air. A series of experiments have been carried out for various combinations of test parameters under atmospheric pressure conditions as summarized in Table 1. The Reynolds number ranges of the condensate and the steam (or steam-air mixture) were about 6 ~ 280 and 416 ~ 6260 (156 ~ 5763), respectively.

3. DATA REDUCTION AND ANALYSIS

3.1 Local Heat Transfer Coefficients

The control volume describing the heat transfer process during reflux condensation is shown in Fig 2. The local condensation heat transfer coefficient (HTC) at any axial location x from the U-tube inlet can be expressed as:

$$h(x) = \frac{q''_{w,i}}{T_b(x) - T_{w,i}(x)} \tag{1}$$

Thus, the local condensation heat transfer coefficient, $h(x)$, is deduced from the measured heat flux $q''_{w,i}$, the temperature T_b at the tube center, and the tube inner wall temperature $T_{w,i}$ at any x.

The heat flux through the tube wall at any axial position x can be calculated from the temperature gradient in the U-tube wall from a steady-state heat conduction equation for a cylindrical geometry, Eq.(2), whereas the tube inner wall temperature can be deduced from the heat flux as given by Eq.(3).

$$q''_{w,i} = k(x)\frac{T_1 - T_2}{r_i \ln(r_2 / r_1)} \tag{2}$$

$$T_{w,i} = T_1 + q''_{w,i}\frac{r_i \ln(r_1 / r_i)}{k(x)} \tag{3}$$

where subscripts 1, 2 denote the radial positions at which thermocouples were installed on the U-tube as shown in Fig.1(c), and the thermal conductivity of tube wall (stainless still 304) $k(x)$ was calculated based on the inner tube temperature measured by a thermocouple.

In the case of a complete reflux condensation, all the injected steam is completely condensed in the U-tube up-flow side. Therefore, the conservation of mass at the steady state yields Eq.(4) and the local mass flow rate of condensate (or steam) can be calculated by Eq.(5) as follows:

$$\dot{m}_g(x) = \dot{m}_f(x) \tag{4}$$

$$\dot{m}_{x+1} = \dot{m}_x - \frac{q_{\Delta x}}{i'_{fg}} \tag{5}$$

where $q_{\Delta x}$ is the heat transfer rate from the primary side to the secondary side of the S/G U-tube between distance Δx and i'_{fg} is the modified latent heat of vaporization considering the effects of the condensate subcooling and the non-linear temperature distribution through the condensate film due to energy convection given by

$$i'_{fg} = i_{fg} + 0.68 C_{p,f} (T_b - T_{w,i}) \tag{6}$$

The definitions of dimensionless parameters used in the present work are as follows:

$$\mathrm{Re}_f = \frac{4\dot{m}_f}{\pi D_i \mu_f}, \quad \mathrm{Re}_g = \frac{4\dot{m}_g}{\pi D_i \mu_g}, \quad \mathrm{Re}_{mix} = \frac{4\dot{m}_{mix}}{\pi D_i \mu_{mix}}$$

$$\mathrm{Ja} = \frac{C_{p,f}(T_b - T_{w,i})}{i_{fg}}, \quad \mathrm{W}_{air} = \frac{\dot{m}_{air}}{\dot{m}_{air} + \dot{m}_g} \tag{7}$$

where μ_{mix} is the viscosity of air-steam mixture and can be calculated by the method of Wilke (1950).

3.2. Flooding Criteria

The most widely used flooding criterion is of the Wallis type flooding correlation and it is expressed as

$$j_g^{*\,1/2} + m\, j_f^{*\,1/2} = C \tag{8}$$

where m and C are empirically determined constants. The parameter j_k^* is a nondimensional superficial velocity of each phase k (f denotes liquid phase and g denotes gas phase) and expressed as

$$j_k^* = j_k \left[\frac{\rho_k}{g\, D (\rho_f - \rho_g)} \right]^{1/2} \tag{9}$$

In the above equation, j_k and ρ_k are the superficial velocity and density of each phase k, D is the diameter of the U-tube, and g is the gravitational acceleration. Wallis et al. (1980) reported that most of their data for air-water and air-steam experiments can be correlated by m = 1, and C = 0.69 ~ 0.8, depending on the entrance geometries.

4. RESULTS AND DISSCUSSION

A series of experiments were performed and a total of 512 data for local condensation heat transfer coefficients (108 for pure steam flow and 404 for steam-air flow conditions, respectively) have been obtained for various inlet flow rates of steam and air. Effect of multiple U-tubes on the onset of flooding has also been examined.

4.1 Heat Transfer Phenomena

4.1.1 Temperature Distributions Along the Tube

The temperature distributions along the tube upflow side with and without noncondensible gas are shown in Figs. 3 and 4, respectively. For the entire experiments, temperature differences between the top and the bottom of the secondary side pool of the S/G were less than 2°C. In the case of pure steam flow, all the injected steam was completely condensed within 1.8m from the tube inlet for the present experimental range, and the temperature change between the active condensation zone and the passive condensation zone was very clear. For the steam-air flow, however, the condensation length was relatively long and the temperature distribution along the tube axial direction tends to decrease gradually due to the effect of noncondensible gas.

4.1.2 Parametric Effects of Pool Temperature and flow rates of Steam and Air on HTCs

The effects of pool temperature and flow rates of steam and air on the heat transfer coefficients (HTCs) are shown in Figs. 5 and 6. From the experimental results shown in Figs. 5 and 6, it can be observed that the condensation length increased when the S/G secondary pool temperature and the flow rates of steam and air were increased.

For the present operating conditions, the ranges of the local heat flux ($q''_{w,i}$) measured at the tube inner wall for pure steam flow and for steam-air flow were ~ 52500 W/m^2 and ~ 49800 W/m^2, respectively. The local HTCs for pure steam flow and for steam-air flow experiments, on the other hand, were found to be around 4940 ~ 27300 W/m^2 K and 120 ~ 6950 W/m^2 K, respectively. As can be observed in Fig. 5, however, in the case of pure steam flow, most of the local condensation HTCs were nearly constant along the tube axial direction with some exceptions, regardless of the steam flow rate and the pool temperature. Fig. 6 shows that, in the case of steam-air flow, the local condensation HTCs increase as the steam flow rate is increased whereas they decrease with increase in the air flow rate.

4.1.3 Development of Empirical Correlation

A total of 512 experimental data for condensation heat transfer coefficients (108 for pure steam flow and 404 for steam-air flow conditions, respectively) have been obtained for various flow rates of steam and air under atmospheric conditions.

In Fig. 7 present experimental data are plotted in the form of HTCs versus the condensate Reynolds number (also steam Reynolds number) for pure steam flows and they are compared with the predictions of representative existing correlations. Although present experimental conditions were different from those assumed in the existing correlations of Nusselt's and Chen's (1961), present data for pure steam flows, in general, agree with theories. At relatively high steam Reynolds number (i.e., larger than 3500), however, the present data is slightly higher than the values predicted by two existing correlations due mainly to the influence of interfacial shear.

In the case of pure steam condensation, the condensate film acts as the only heat transfer resistance, whereas when noncondensible gases are present, the liquid-steam interface where noncondensible gases carried by the

steam is being accumulated becomes the main resistance to heat transfer. To quantify the parametric effects of flow rates of steam and noncondensible gases (air) on the heat transfer coefficient, therefore, a new correlation applicable to the reflux condensation mode has been developed using the degradation factor concept based on the steam-air experimental results.

The degradation factor, F, is a correction factor to the local heat transfer coefficient based on Nusselt theory, i.e., it is defined as the ratio of the local experimental condensation heat transfer coefficient (h_{exp}) to the local theoretical Nusselt value (h_f). The value of h_f is defined by Eq.(10) and the condensate film thickness δ is calculated from Eq.(11) as follows:

$$h_f = \frac{k_f}{\delta} \tag{10}$$

$$\delta = \left[\frac{4\mu_f k_f z(T_{g,i} - T_w)}{g i_{fg} \rho_f (\rho_f - \rho_g)}\right]^{1/4} = \left[\frac{3\mu_f{}^2 \,\mathrm{Re}_f}{4\rho_f (\rho_f - \rho_g) g}\right]^{1/3} \tag{11}$$

The local HTCs can be considered to be principally a function of the steam-air mixture Reynolds number Re_{mix}, the air mass fraction W_{air} (which accounts for the presence of noncondensible gas) and Jacob number. The correlation was developed using a least-square fit method as follows:

$$F = \frac{h_{\exp}}{h_f} = 3.2\times10^{-5}\ \mathrm{Re}_{mix}^{0.75}\ \mathrm{W}_{air}^{-0.45}\ \mathrm{Ja}^{-0.70} \tag{12}$$

The ranges of application for Eq. (12) are :

$$156 < \mathrm{Re}_{mix} < 5673,$$
$$0.030 < \mathrm{W}_{air} < 0.865,$$

and

$$0.017 < \mathrm{Ja} < 0.133.$$

The measured HTCs are compared with the values obtained by Eq.(12) in Fig. 8. With some exceptions, most of the present data agree with predicted values within ±30% as can be seen in Fig. 8.

4.1.4 Comparison of the Present Data with the Existing Correlation

In Fig. 9, on the other hand, present experimental data are compared with the existing correlation of Moon et al. (2000). Moon et al.'s study was carried out using a single vertical tube (16.56mm-i.d. and 2.4m-length.) surrounded by a concentric coolant jacket (57.2mm-i.d). The steam flow rate is comparable to the present work, but inlet air mass fractions used in their experiments (11.8~55%) are relatively higher than those of the present (1~24%). The definitions of dimensionless parameters used in both experiments are the same, and therefore a direct comparison between the two is possible.

As can be seen in Fig. 9 the present experimental data are slightly higher (38.5% in average) than the values predicted by Moon et al.'s correlation. Main reasons for this may be due to the following: First, there is appreciable difference in the inlet air mass fraction between the present and theirs. Secondly, the local heat flux through the U-tube wall of the present work was evaluated from the temperature gradient at the tube wall, whereas that of Moon et al.'s was evaluated using the rate of increase in secondary side coolant temperature between adjacent thermocouples.

4.1.5 Uncertainty Analysis

The uncertainty of measured heat flux values is examined by comparing the enthalpy inflow (steam mass flow rate multiplied by steam enthalpy) and the heat flux integrated over the U-tube height (condensation length). The maximum uncertainty of the height averaged heat flux was 17.9%. The uncertainty analysis for the local HTCs has also been carried out by the following error propagation method:

$$\sigma^2(h) = \left(\frac{\partial h}{\partial q''_{w,i}}\right)^2 \sigma^2(q''_{w,i}) + \left(\frac{\partial h}{\partial T_b}\right)^2 \sigma^2(T_b) + \left(\frac{\partial h}{\partial T_{w,i}}\right)^2 \sigma^2(T_{w,i})$$

$$\frac{\sigma(h)}{h} = \left[\left(\frac{\sigma(q''_{w,i})}{q''_{w,i}}\right)^2 + \left(\frac{\sigma(T_b)}{T_b - T_{w,i}}\right)^2 + \left(\frac{\sigma(T_{w,i})}{T_b - T_{w,i}}\right)^2\right]^{1/2} \tag{13}$$

The error of the tube centerline temperature (T_b) was 0.8 °C and those of local heat flux ($q''_{w,i}$) and tube inner wall temperature ($T_{w,i}$) can also be calculated by the error propagation method using Eqs.(2) and (3). The estimated uncertainties of HTCs were in the range of 2.4 ~ 19.7% and these uncertainties were mainly resulted from the error of thermocouples. The detailed results are summarized in Table 2.

4.2 Flooding Phenomena

4.2.1 Onset of Flooding in Multiple U-tubes

Fig. 10 shows present experimental results of flooding phenomena in multiple U-tubes of different lengths (two long tubes and two short tubes) during a reflux condensation. The steam was injected into the four U-tubes by passing through an inlet plenum. To obtain the steam flow rate for each U-tube, the condensate mass flowing out from each tube was measured. When the outlet plenum was open to the atmosphere, there was no tendency for steam to flow into any particular tube and the observed flow pattern in each of the four U-tubes was about the same.

The results also showed that the height of U-tube and the condition of the secondary side had negligible effects on the onset of flooding. As can be seen in Fig. 10, the present flooding data generally agree with Wallis-type flooding criterion (with m = 1, C = 0.87~1.0). However, the flooding occurred at lower steam flow rate per U-tube when the number of U-tubes was increased: The range of C values were different depending on the number of U-tubes (i.e., 0.95~1 for single U-tube, 0.9~0.93 for two U-tubes and 0.87~0.92 for four U-tubes,

respectively). The reason for this may be due mainly to the tube entrance effect since there was no tendency for steam to flow into any particular tube.

4.2.2 Comparison of Present Flooding Data with Previous Results

The present flooding data are compared with the results of Chen et al. (1999) and Moon et al. (2000) in Fig.11. Chen et al. (1999) carried out their flooding experiment for reflux condensation in a single inverted U-tube (D = 20mm, H = 4.1m and 7.0m) without noncondensible gas, whereas Moon et al. (2000) performed their experiment in a single vertical tube (D = 16.56mm, H = 2.4m) with noncondensible gas (inlet air mass fraction was 13~37%).

As can be seen in Fig.11 there is appreciable difference between the present flooding data and the results of Chen et al. and Moon et al. The main reason for this discrepancy may be attributable to the difference in experimental conditions used such as the tube diameter, entrance geometry, noncondensible gas fractions, and the system pressure.

5. CONCLUSIONS

A series of experiments were performed and a total of 512 data for local condensation heat transfer coefficients (108 for pure steam flow and 404 for steam-air flow conditions, respectively) have been obtained for various inlet flow rates of steam and air. Effects of multiple U-tubes with different lengths and noncondensible gases on the onset of flooding during a reflux condensation have been examined. From the results of the present work following conclusions can be made.

(1) When only steam was flowing, most of the local condensation HTCs were nearly constant (~7500 W/m^2K) along the tube axial direction with some exceptions, regardless of the steam flow rate and the pool temperature. However, when noncondensable gases were present, as in the case of steam-air flow, the local condensation HTCs increased as the steam flow rate was increased, whereas they decreased with increase in the air flow rate.

(2) Present experimental results obtained for pure steam flows, in general, agree with the existing correlations of Nusselt and Chen (1961). At relatively high steam Reynolds number (i.e., larger than 3500), however, the present data is slightly higher than those values predicted by two existing correlations due mainly to the influence of interfacial shear.

(3) To include the effects of flow rates of steam and noncondensible gases (air) on the heat transfer coefficient, a new correlation applicable to the reflux condensation mode has been developed using the concept of degradation factor based on the steam-air experimental results. The degradation factor, F, is a correction factor to the local heat transfer coefficient based on the Nusselt theory, and it is defined as the ratio of the local experimental condensation heat transfer coefficient (h_{exp}) to the local theoretical Nusselt value (h_f). The degradation factor is

correlated in terms of the steam-air mixture Reynolds number, air mass fraction, and the Jacob number as given by Eq. (12).

(4) The effect of multiple U-tubes with different lengths (i.e., two-short and two-long U-tubes) on the onset of flooding during a reflux condensation has also been examined. When the outlet plenum was open to the atmosphere, there was no appreciable difference in the steam flow rate among the multiple U-tubes and the height of U-tube and the condition of secondary side had negligible effect on the onset of flooding. The present flooding data generally agree with Wallis-type flooding criterion (with m = 1, C = 0.87~1.0). However, the flooding occurred at lower steam flow rate per U-tube when the number of U-tube was increased due mainly to the flow instability and tube entrance effect.

NOMENCLATURE

C	constant in Eq. (8)
D	tube diameter (m)
g	gravitational acceleration (m/s^2)
H	height of U-tube (m)
h	heat transfer coefficient (W/m^2K)
i	enthalpy (J/kg)
j	superficial velocity (m/s)
Ja	Jacob number
k	thermal conductivity (W/m K)
M	molecular weight
m	constant in Eq. (8)
$\dot{m}$	mass flow rate (kg/s)
P	pressure (Pa)
Pr	Prandtl number
q	heat transfer rate (W)
q''	heat flux (W/m^2)
r	tube radius (m)
Re	Reynolds number
T	temperature (^oC)
W	air mass fraction (AMF)
x	mole fraction

Greek

δ	condensate film thickness
μ	viscosity (Ns/m^2)

ρ density (kg/m^3)

σ uncertainty

Subscript

f liquid(condensate) phase

g gas(steam) phase

i tube inner side

mix steam-air mixture

w tube wall

1 inner T/C location

2 outer T/C location

Δx distance between thermocouples

Superscript

* dimensionless quantity

REFERENCES

[1] Banerjee, S., Chang, J-S., Girard, R., and Krishnan, V. S., "Reflux Condensation and Transition to Natural Circulation in a Vertical U-Tube," J. Heat Transfer, Vol. 105, pp. 719-727, 1983.

[2] Chen, H. Y., Chen, Y. Z., and Zang, Z. Y., "Investigation of Reflux Condensation in Single Inverted U-tubes," Ninth International Topical Meeting on Nuclear Reactor Thermal Hydraulics (Nureth-9), San Francisco, California, October 3-8, 1999.

[3] Chen, M. M., "An Analytical Study of Laminar Film Condensation: Part 1 – Flat Plates," J. of Heat Transfer, Vol. 83, pp. 48-54, 1961.

[4] Chou, G. H. and Chen, J. C., "A General Modeling for Heat Transfer During Reflux Condensation Inside Vertical Tubes Surrounded by Isothermal Fluid," Int. J. Heat Mass Transfer, Vol. 42, pp. 2299-2311, 1999.

[5] Chun, M. H. and Park, J. W., "Reflux Condensation Phenomena in Vertical U-tubes With and Without Noncondensible Gases," ASME Paper No. 84-WA/HT-2, 1984.

[6] Moon, Y. M., NO, H. C., Park, H. S., and Bang, Y. S., " Assessment of RELAP5/MOD3.2 for Reflux Condensation Experiment," Report NUREG/IA-0108, 2000.

[7] Vierow, K. M. and Schrock, V. E., "Condensation in a Natural Circulation Loop With Noncondensable Gases

PART I - Heat Transfer," Proc. The International Conference on Multiphase Flows, Tsukuba, Japan, September 24-27, 1991.

[8] Wallis, G. B., Desieyes, P. C., Roselli R. J., and Lacombe, J., "Countercurrent Annular Flow Regime for Steam and Subcooled Water in a Vertical Tube," EPRI/NP-1336, 1980.

[9] Wilke, C. R., "A Viscosity Equation for Gas Mixtures," J. Chemical Physics, Vol. 18, No. 4, pp. 517-519, 1950.

Table 1 Test Matrix of the Present Experiment

Experiment		Pool Temp. (°C)	Steam Flow Rate (LPM)	Air Flow Rate (LPM)	Air Mass Fraction (%)	Re_f (j_f^*)	Re_g (j_g^*)	Re_{mix}	No. of Data
Condensation Heat Transfer	Pure Steam	40 ~ 75	30 ~ 100	•	•	6.1 ~ 272	416 ~ 6260	•	108
	Steam-Air	25 ~ 40	30~ 100	1 ~ 10	3.0 ~ 86.5	15 ~ 258	•	156 ~ 5763	404
Flooding		45 ~ 85	Up to flooding	•	•	(0.014 ~ 0.019)	(0.6 ~ 0.75)	•	6 for single tube 3 for two-tubes 4 for four-tubes

Table 2 Parameters and Estimated Uncertainties

	Parameters	Uncertainty	Average Value
Independent Parameters	Temperature	0.8°C	
	Position error of T/C	0.003 m	
Dependent Parameters	Heat Flux	9.3 ~ 47.7%	17 %
	Inner Wall Temperature	0.84~1.55°C	1.16 °C
	Local HTCs	2.4 ~ 19.7%	8.3 %

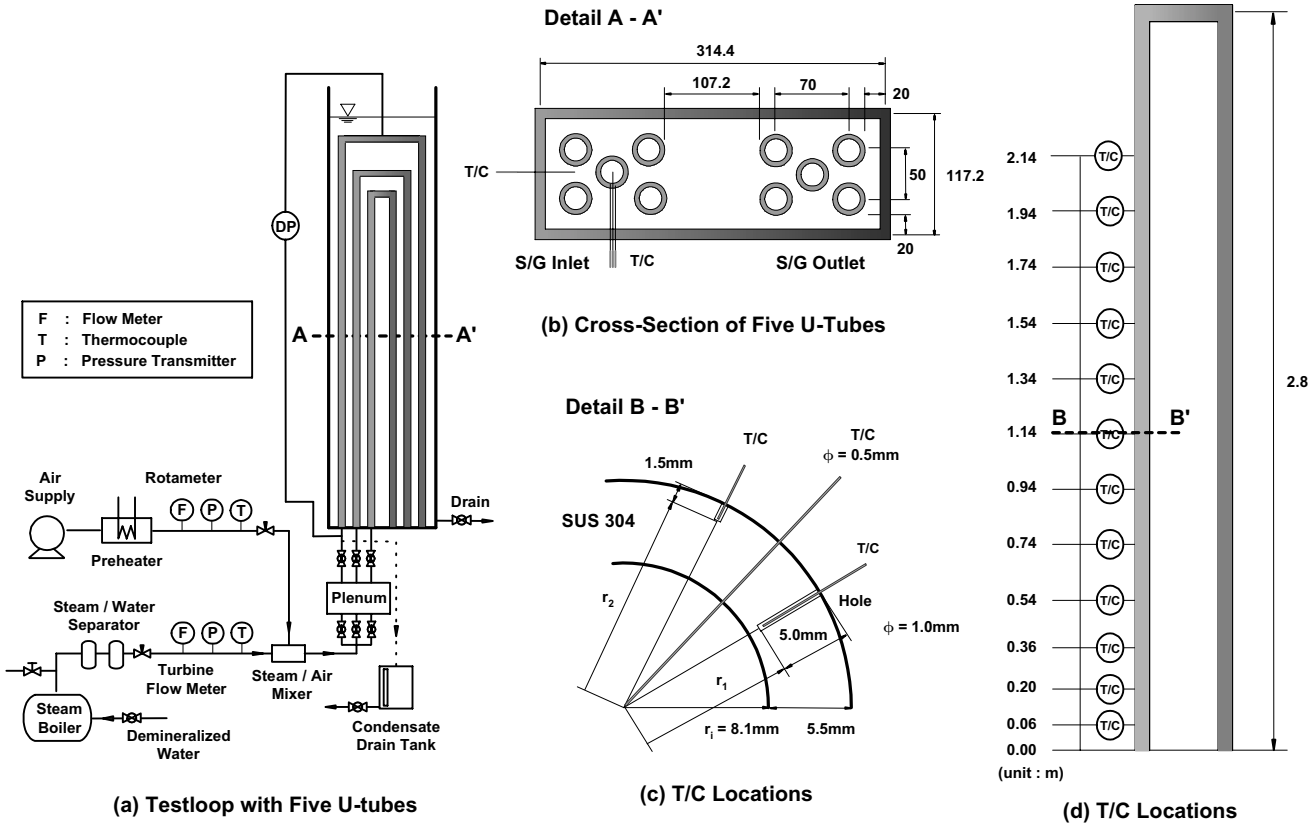

Fig. 1 Schematic Diagram of Experimental Apparatus

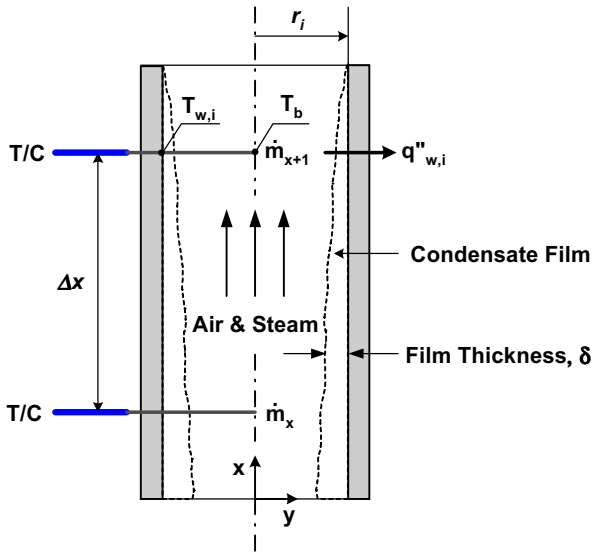

Fig. 2 Control Volume for Reflux Condensation

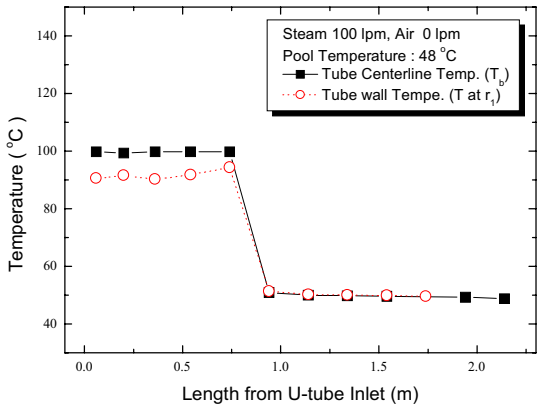

Fig. 3 Temperature Profiles Along the Tube in the Absence of the Noncondensible Gas

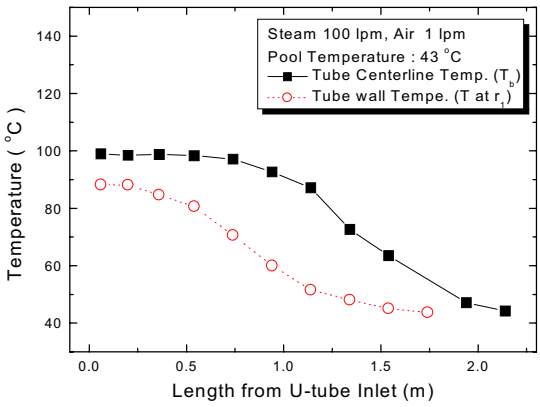

Fig. 4 Temperature Profiles Along the Tube in the Presence of the Noncondensible Gas

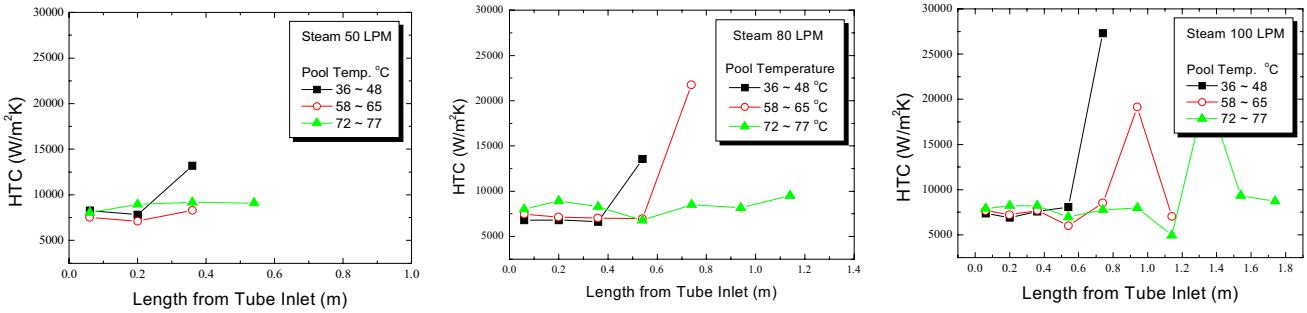

(a) Steam Flow Rate : 50 LPM (b) Steam Flow Rate : 80 LPM (c) Steam Flow Rate : 100 LPM

Fig. 5 Effects of Pool Temperature and Steam Flow Rate on the Heat Transfer Coefficients With Pure Steam

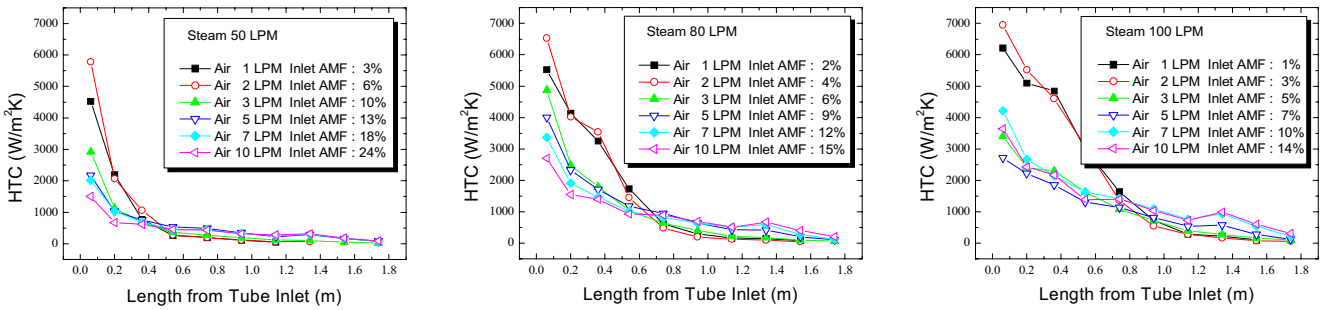

(a) Steam Flow Rate : 50 LPM (b) Steam Flow Rate : 80 LPM c) Steam Flow Rate : 100 LPM

Fig. 6 Effects of Pool Temperature and Steam and Air Flow Rates on the Heat Transfer Coefficients With Noncondensible Gas

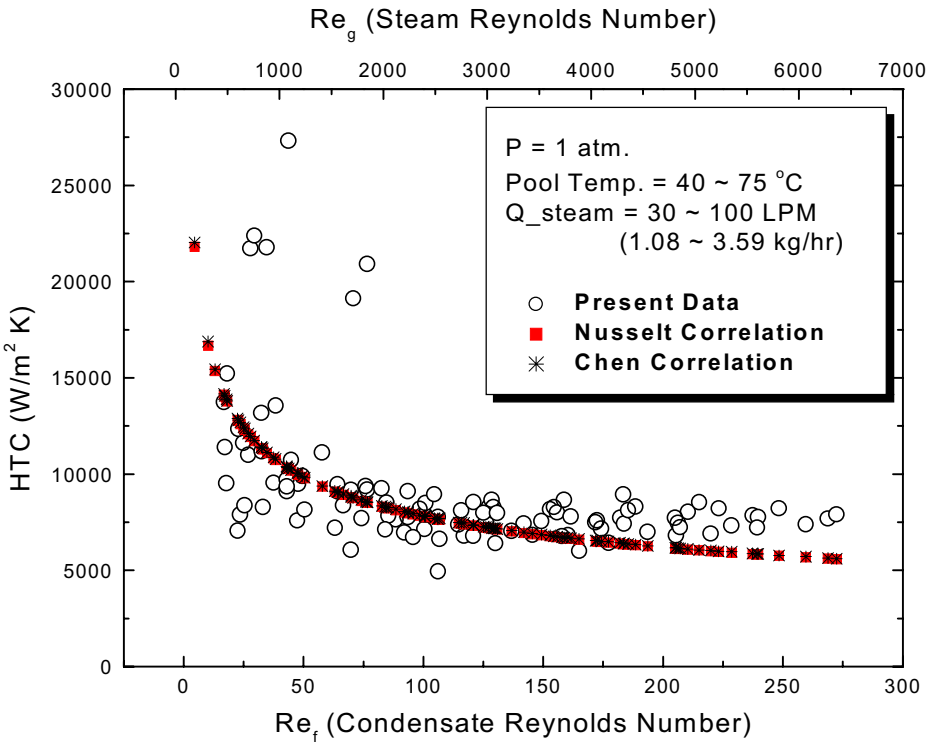

Fig. 7 Comparison of the Experimental Data with Existing Theories in the Absence of Noncondensible Gas

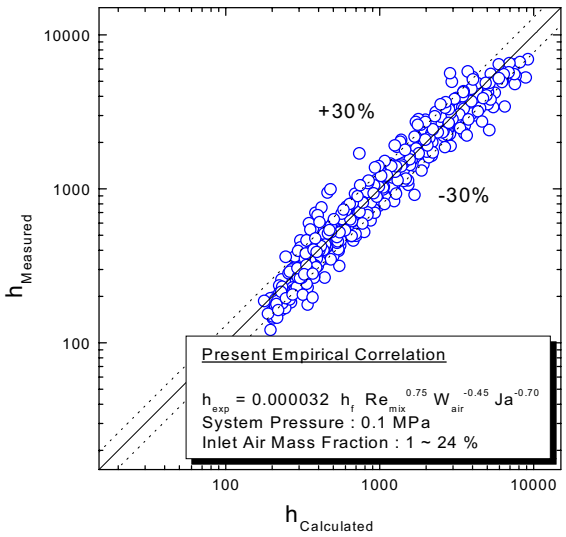

Fig. 8 Comparison of Measured HTCs with Calculated HTCs

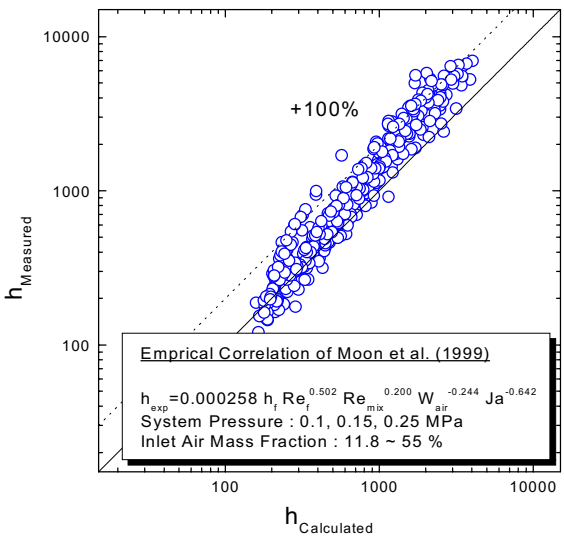

Fig. 9 Comparison of the Present Experimental Data with Existing Correlations in the Presence of Noncondensible Gas

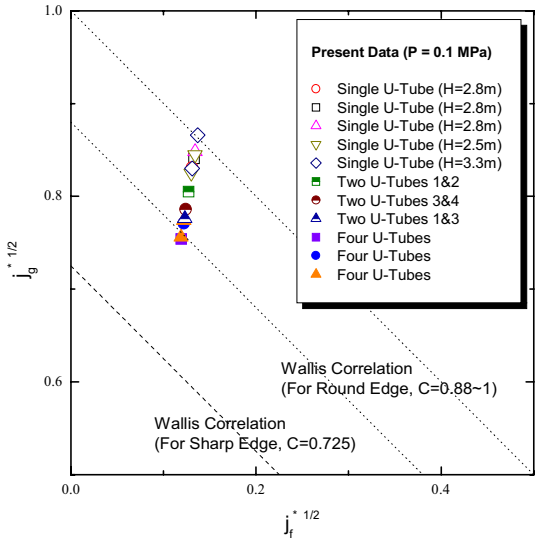

Fig. 10 Present Experimental Data for Onset of Flooding in Multiples U-tubes

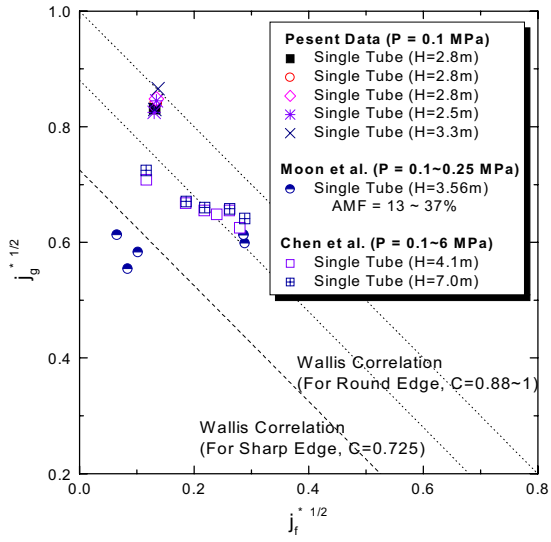

Fig. 11 Comparison of Present Flooding Data with Existing Data of Chen et al. and Moon et al.